More coherent noise attenuation in the radial trace domain

David C. Henley

ABSTRACT

The radial trace (R-T) domain has been shown to be useful for coherent noise attenuation and other seismic wavefield separation operations because of the particular geometric distortion produced by the R-T transform. In recent work, a number of different variations of R-T domain coherent noise attenuation were tested and compared using a familiar shot gather from the Blackfoot seismic survey. The more promising methods are identified.

Because the R-T transform does not require input data to be uniformly gridded, R-T domain coherent noise attenuation can be readily applied to appropriate trace gathers from 3D land data sets. For most surveys, receiver line gathers are the most appropriate trace ensembles for coherent noise attenuation.

The R-T software modules in ProMAX have been updated to reflect recent work and to assist in testing proposed new R-T operations. These alterations are described and documented.

INTRODUCTION

Radial trace domain techniques for attenuating coherent noise in seismic data were introduced by Henley (1999; 2000; 2003), based partly on earlier work by Claerbout (1975; 1983), who introduced the radial trace (R-T) transform primarily for use in migration and related imaging algorithms. R-T coherent noise attenuation techniques rely on the fact that separation of linear noise from reflections can be achieved in the radial trace domain by aligning the transform coordinate trajectories with the coherent noise wavefronts in the X-T domain. As a result, linear noises projected across many constant-offset traces of an X-T gather are collapsed into narrow groups of constant-velocity traces in the R-T domain. Furthermore, the apparent frequencies of these events drop significantly, often to the sub-seismic range (Henley, 1999). This latter effect in particular can be utilised to separate coherent noise from the rest of the wavefield expressed on a seismic shot gather. One of two approaches can be used to accomplish R-T domain coherent noise attenuation. The noise can be suppressed directly by applying a low-cut filter to the R-T domain traces, then transforming back to the X-T domain. Alternatively, the noise can be estimated or 'modelled' by applying a low-pass filter to the R-T domain traces followed by the inverse R-T transform. The resulting X-T domain estimated noise can then be directly subtracted from the original shot gather. The latter approach has proved to be more flexible and more generally effective, so the 'model-and-subtract' technique is the one used for most of the results shown here.

It has been shown that the interpolation method used in the discrete R-T transform greatly influences the relative fidelity with which reflection-like events and linear noise are mapped by the transform (Claerbout, 1983), (Brown and Claerbout, 2000). In

particular, interpolation in the X-direction preserves reflections but not some coherent noise, especially spatially aliased noise. Interpolation along R-T trajectories (V-interpolation), however, favours any coherent noise aligned with the R-T trajectories but can alias reflections. Experience has shown that V-interpolation is particularly useful when using the R-T dip transform configuration to model low-velocity, spatially aliased noises such as air blast. V-interpolation has been documented elsewhere (Henley, 2002) and will not be investigated further here.

The 'model-and-subtract' method of coherent noise attenuation readily lends itself to optimization of both the modelling and the subtraction operations. Among the questions arising for the subtraction phase are:

- Should the noise estimate be scaled before subtraction?

- If so, should the scaling be constant for the gather, or should it depend upon some trace-by-trace measure of S/N?

- Can the estimation and subtraction method be iterated?

- If so, how many iterations are best?

The key issue for estimating or 'modelling' linear noise from the full wavefield in the R-T domain is how to most effectively isolate the part of the wavefield that constitutes the linear noise from the part considered to be 'signal'. Previously, the only operation used routinely for this purpose has been the low-pass zero-phase Ormsby filter. Conceivably, however, there are other single and multi-trace operations which could be equally suitable or even superior for wavefield component separation in the R-T domain:

- Single-channel filters including running mean (boxcar filter), running median, weighted running mean, etc.

- Multi-channel filters including K-F filter, 2D boxcar filter, relative trace scaling, combined trace mix/low-pass filter, etc.

MODELLING AND REMOVING COHERENT NOISE

Single-trace operations

The R-T transform isolates coherent noise by velocity and frequency, so any single-trace operation which selectively attenuates seismic frequencies can be used in the 'modelling' or estimation of the R-T domain coherent noise, as can any single-trace operation which alters output trace amplitudes relative to neighbouring traces. The inverse R-T transform of the model then yields an X-T domain noise estimate which can be subtracted from the input gather. The most obvious single-trace operation to use is some form of low-pass frequency filter such as a zero-phase Ormsby filter, which will be illustrated first and used as the standard for comparison with later results. Figure 1 shows a generic shot gather from the Blackfoot seismic survey, which will be used for all the results reported here, while Figure 2 shows its R-T fan transform with respect to the

apparent source point (the origin of the R-T transform is the intercept of the direct arrival with the zero offset axis). A low-pass filtered version of the R-T transform appears in Figure 3, while the inverse R-T transform of this filtered transform is shown in Figure 4. This estimate of the coherent noise in the original shot gather looks quite reasonable to the eye—no apparent reflection energy. Nevertheless, when it is subtracted, with a coefficient of unity, from the input, residual coherent noise is still present (Figure 5), indicating some potential for improvement of the technique, either in the subtraction process or the modelling. Weighting the noise estimate more heavily (a coefficient of 1.25) results in Figure 6, while a smaller factor of 0.8 yields Figure 7. Comparing both Figures 6 and 7 with Figure 5 shows, through their similarity, that the method is not particularly sensitive to the value of this coefficient, although the direct arrivals seem slightly better attenuated in Figure 6. Figure 5, with its subtraction coefficient of unity, will represent the standard 'model-and-subtract' results for comparison with all other results shown here.

In an attempt to optimise noise subtraction, various schemes were tested; including (1)—weighting the individual noise estimate traces in the X-T domain by the reciprocal of their S/N ratio with respect to their corresponding unfiltered X-T domain input traces; (2)—trace amplitude equalisation of the noise estimate traces in the R-T domain; and (3)—trace amplitude equalisation of both the input gather and the noise estimate in the R-T domain before subtraction in the X-T domain. None of the methods tested showed any visible improvement over a single, constant multiplicative factor slightly greater than unity applied to the entire noise estimate panel. One possible approach *not* tested, however, is that of finding, for each X-T domain noise estimate trace, the factor which minimises the squared difference between the corresponding input trace and the scaled noise estimate trace (assuming that noise dominates each input trace). Further investigation of subtraction techniques remains.

Since a single pass of the model-and-subtract procedure always leaves some residual noise, can iterations of the same procedure remove more noise? Using the result shown in Figure 5 as the input and repeating the same model-and-subtract R-T filter pass, the resulting estimated noise is as shown in Figure 8, after AGC. Subtracting this noise estimate from the gather in Figure 5 yields the results in Figure 9, clearly an improvement. Figure 10 shows the noise estimated from the fourth iteration of the procedure, while the significantly improved gather is shown in Figure 11. Testing has shown that improvement continues up through four or five iterations but diminish rapidly thereafter. Interestingly, it also appears that when using the model-and-subtract method iteratively, the value of the subtraction coefficient is even less important. Evidently, if an inappropriate coefficient choice results in more residual noise on the first pass, subsequent estimation and subtraction will reduce this residual, so that by the fourth iteration, results are indistinguishable for significantly different values of coefficient.

A question raised by the success of iteration is whether four discrete iterations of model-and-subtract gives a better result than simply modelling with four sequential low-pass filters in the R-T domain and one subtraction operation in the X-T domain. Figure 12 shows the noise estimate resulting from four consecutive passes of a low-pass filter on the R-T domain shot gather, while Figure 13 contains the result of subtracting this

estimate in the X-T domain and should be compared to Figure 11. Clearly, the discretely iterated model-and-subtract results in Figure 11 are superior.

In addition to the subtraction operation, the other major aspect of the model-and-subtract technique is the estimation or 'modelling' of the noise from the R-T transform of the input. This is normally done by isolating the noise by apparent frequency and/or velocity in the R-T domain. There are a number of single and multi-trace operations that can provide this frequency/velocity separation.

So far, the only single-trace frequency discrimination operation demonstrated here for separating coherent noise from signal in the R-T domain is the zero-phase low-pass Ormsby filter. Are there other single-trace operations that perform as well or better? For example, Figures 14, 16, and 18 show reasonable-looking coherent noise estimates made using a running mean (boxcar) operator on the R-T domain traces of Figure 3, with operator lengths of 100, 50, and 25 points. Figures 15, 17, and 19 contain the results of subtracting each of these noise estimates, respectively, from the original shot gather. The best of these results appears to be the one using the 25-point running mean, both in terms of reflection coherence and bandwidth. However, reflection energy can be seen leaking into the noise estimate in Figure 18, so the reflection fidelity in Figure 19 may be compromised by some subtracted reflection energy. The frequency response of the running mean is known to have relatively high side lobes and would not be expected to produce as clean a frequency discrimination as the Ormsby filter. Cascading a boxcar filter two or more times, however, diminishes the spectral side lobes and improves spectral isolation. Figure 20 shows the coherent noise estimate resulting from three passes of the 50-point running mean filter (basically a weighted 150-point running mean). When this noise estimate is compared with that in Figure 16, it can be seen that there is much less apparent leakage of reflection energy. Subtracting the noise estimate in Figure 20 from the shot gather results in Figure 21; this can be compared to Figure 17. Although the reflections seem to have more bandwidth (less ringing), coherence is no better, and actual S/N may not be as good as on Figure 17. None of the running mean results (Figures 15, 17, 19, and 21) appear in any way superior to those produced using a simple zero-phase Ormsby low-pass filter to estimate the coherent noise (Figure 5).

Non-linear operations can sometimes be more effective than comparable linear operations, if the non-linearity itself does not lead to unacceptable artefacts. For this reason, it was decided to test the running median as a high-frequency discriminator, to see whether it could more effectively separate the low-frequency coherent noise from signal than the Ormsby low-pass filter. Figures 22, 23, and 24 show coherent noise estimates made using the running median on R-T domain traces of Figure 3, with operator lengths of 100, 50, and 300, respectively. Close examination of all three noise estimates shows evidence of artefacts due to non-linearity. For example, clipping appears in the centre traces of Figure 22, and various high-frequency artefacts can be found scattered throughout Figures 23 and 24. The best of these estimates appears to be the one resulting from the 300-point running median, so Figure 25 shows the result of subtracting that estimate from the input gather. This result appears no better than earlier results using the Ormsby filter or running mean.

Multi-trace operations

One rationale for restricting R-T domain operations to single traces is to ensure the invertibility of the R-T transform in order to accurately reconstruct the X-T reflection wavefield. However, this constraint applies mainly when attenuating noise directly in the R-T domain. If the R-T domain is being used only to model the noise, there is no reason to exclude multi-trace operations like K-F filtering or other 2D smoothing operations for accomplishing the extraction of noise from the R-T wavefield.

Figure 26 shows the result of applying a K-F filter in the R-T domain to model the low-velocity, low-frequency linear noise. The filter parameters were chosen, with considerable trial and error, by measuring the apparent dips of noise events present on the R-T transform of the shot gather (Figure 2). It should be noted that a K-F transform of R-T space will have a different meaning than a transform of X-T space, since the dimensions of R-T coordinates are velocity and time, rather than distance and time. A linear slope in this new hybrid K-F domain will therefore have units of 'acceleration' rather than velocity. As in previous examples, the coherent noise appears to be well modelled, but some visible reflection energy leaks into this noise estimate. It is no surprise, therefore, that the result of subtracting this noise estimate from the input gather, as shown in Figure 27, shows much improved reflection coherence, but also somewhat reduced reflection bandwidth. Nevertheless, the results appear better than most other results shown thus far, including the single-trace Ormsby low-pass filter with similar frequency response (Figure 5). To further test the use of a K-F filter in the R-T domain, Figure 28 shows the result of applying a K-F filter whose characteristics make it the complement of that used to model the coherent noise. As can be seen, this filter is very effective in attenuating the coherent noise, but the price of this effectiveness is the lateral smearing of traces, most evident at longer times (for example, the 60 Hz noise trace in the right-hand part of the spread). Since there is no smearing with the model-and-subtract method, that result (Figure 27) is the preferred one.

Other operations or combinations of operations have potential as multi-trace noise discriminators in the R-T domain. Perhaps the simplest possibility is the 2D boxcar filter, comprised of a running mean applied to single R-T traces and an unweighted running trace mix applied to the R-T gather. A noise estimate obtained using a 50-point running average and 9-trace running mix is shown in Figure 29, and the result of subtracting this noise estimate shown in Figure 30. Combining an Ormsby filter with a weighted trace mix results in the noise estimate shown in Figure 31; and the result of subtracting this estimate is displayed in Figure 32. Neither of these results appears to show any advantage with respect to single-trace operations already demonstrated; but it is quite likely that other multi-trace operations can be devised which do demonstrate better performance than single-trace ones, as did the K-F filter.

The feature of the R-T transform that is most important to effective separation of linear modes from the rest of the wavefield is the parametric control of the local orientation of the radial trace trajectories with respect to the underlying coherent noise wavefronts. In many cases, the actual coherent noise wavefronts are not exactly linear and thus will not conform properly to linear R-T trajectories. In other cases, spatial aliasing of low-velocity events in the X-T domain precludes their proper sampling along

conformable R-T trajectories. In the first case, R-T trajectories can be made *more* conformable to the underlying noise wavefronts by slightly curving them upwards. In the other case, making the R-T trajectories *less* conformable by curving them downwards can reduce the aliasing and improve the fidelity with which noise events are mapped. Figure 33 shows the radial fan transform of the Blackfoot shot gather using the usual linear R-T trajectories; figure 34 shows the transform resulting from applying downward curvature to the R-T trajectories (20% decrease per second from initial velocity); and the transform in Figure 35 has trajectories with 50% increase per second from initial velocity. The differences in orientation of the linear events in these transforms with respect to the reflections are subtle but significant for filtering. To illustrate, the same low-cut Ormsby filter has been applied to all three transforms before inversion. Figures 36, 37, and 38 show the results for the linear R-T trajectories, upward-curved, and downward-curved trajectories, respectively. The slightly improved noise attenuation observed in Figure 37 is due to the better fit of the R-T trajectories to coherent noise wavefronts, while the more substantial improvement observed in Figure 38 is due to reduced spatial aliasing in this modified   R-T transform.

3D NOISE ATTENUATION

Even in the earliest description of coherent noise attenuation in the R-T domain, it was recognised that using the technique on 3D seismic data might be one of its more useful applications, since other 3D methods are tedious (usually requiring regularising the data to a uniform grid) and often ineffective. While some R-T noise attenuation had been applied to 3D data in the past, a number of issues had not been thoroughly investigated until this past year at the request of some CREWES sponsors. Probably the most significant question for effective noise attenuation in the R-T domain (or any other domain) is how to organise the traces within a 3D shot gather to maximise the noise attenuation while minimising the number of R-T filter passes per shot. After extensive experimentation with various trace panels extracted from 3D land shot gathers (receiver line gathers, constant azimuth gathers, constant radius gathers, cross-spreads, etc.), the following reflects current CREWES views on 3D R-T coherent noise attenuation:

- For most 3D land surveys, receiver line gathers are the most densely spatially sampled trace gathers; and shot-generated noise is most coherent and least aliased on those gathers. Coherent noise attenuation is most effective when applied to these gathers. Most attempts to construct a 'supergather' from all the traces in a shot, in order to apply a single R-T filter pass to each shot, destroy at least some of the spatial coherence of the noise, making the filtering less effective.

- The 'signed offset' trace header, used by the *radial filter* module, has no meaning in the 3D geometry context. This trace header must be assigned to all traces prior to noise attenuation so that in the portion of each receiver line gather for which absolute offset decreases with channel number, the signed offset header equals the negative of the absolute offset; while in the portion of the gather where absolute offset increases, the signed offset header equals the absolute offset. This trace header trick makes each 3D receiver line gather

appear to be a split-spread shot gather (with a non-linear offset distribution), which can then be easily processed with the CREWES *radial filter* or *radial trace transform*.

As an illustration of the effectiveness of R-T domain noise attenuation in 3D, Figure 39 shows two receiver line gathers from a 3D land data set, both heavily contaminated with source-generated noise. The noise appears non-linear due to the very non-uniform distribution of source-receiver offsets within each gather. Figure 40 shows the same gathers after R-T domain noise estimation and subtraction. The non-uniform offset distribution poses no problem for the R-T transform.

PROMAX MODULE MODIFICATIONS

For the previous CREWES versions of both *radial filter* and *radial trace transform* modules in ProMAX, the so-called 'V-interpolation' option could only be accessed by choosing the number of radial traces to be a multiple of three. This awkward feature has now been removed, and V-interpolation is now one of the options selectable under the 'Interpolation method' parameter.

In the previous version of *radial filter*, the default filter type was 'subtract low-pass in X-T', the new version has the same default, but now also includes a new parameter for this choice; a 'subtraction coefficient' or scalar which multiplies the noise estimate before subtraction from the input gather. The default value of this scalar is unity, but other values can be useful, particularly when using *radial filter* iteratively.

Since the *radial filter* module maintains a complete internal representation of the input X-T trace panel, the original panel, with regions modified by filtering in the R-T domain, can be easily reconstructed for output. The *radial trace transform* module itself, however, has no such provision, since the forward output consists solely of radial traces (usually for diagnostic purposes), with mostly dummy trace headers. It may sometimes be desirable to transform radial traces back to the X-T domain, however. The new version of the *radial trace transform* module stores the minimum and maximum X-T domain offset values in the unused SOU_X and REC_X trace headers, respectively, of the radial traces. When the inverse transform is initiated, default (zero) values of minimum and maximum offset parameters cause the algorithm to use the R-T trace header values in SOU_X and REC_X in order to restore the original *range* of offsets for the X-T panel. No matter what the actual distribution of offsets in the original X-T panel, however, the output panel will have linearly distributed offsets (or, optionally, quadratically distributed offsets). In fact, one use of the R-T transform and its inverse is to regularize an input gather that has offset values that vary significantly from linearity.

CONCLUSIONS

The technique of R-T filtering has been advanced by new experience as well as by software corrections and enhancements, including a new interpolation method for the R-T transform itself, that allows a better estimate of some linear noises, especially low-velocity partially aliased linear noise. Subtraction of noise modelled in the R-T domain appears to be the most generally applicable technique for coherent noise removal.

A number of single and multi-trace operations can be used in the R-T domain to affect the modelling of coherent noise (mapped into constant velocities and low frequencies), but the most effective single-trace operation appears to be the simple low-pass Ormsby filter. The multi-trace K-F filter can be even more effective, but some design trial and error may be required. The subtraction coefficient used with various noise estimates appears not to be particularly sensitive. One modification of the technique that appears to be worthwhile is to iterate the model-and-subtract cycle as many as four times with the same R-T transform and filter parameters. In this case, the choice of subtraction coefficient becomes nearly irrelevant.

Another way to improve the performance of R-T filtering is to alter the R-T trajectories themselves in order to either improve conformity with noise wavefronts on shot gathers, or to decrease aliasing (these may be mutually exclusive, depending upon the particular data set). An interesting challenge is to develop an algorithm that would produce R-T trajectories that adaptively track noise wavefronts.

ACKNOWLEDGEMENTS

REFERENCES

Brown, M., and Claerbout, J.F., 2000, A pseudo-unitary implementation of the radial transform, 70th Ann. Internat. Mtg. Soc. Expl. Geophys., Expanded Abstracts.
Claerbout, J.F., 1975, Slant-stacks and radial traces, Stanford Exploration Project Report, SEP-5, 1-12.
Claerbout, J.F., 1983, Ground roll and radial traces, Stanford Exploration Project Report, SEP-35, 43-53.
Henley, D.C., 1999a, Coherent noise attenuation in the radial trace domain: introduction and demonstration, CREWES Research Report Vol. 11.
Henley, D.C., 1999b, Demonstration of radial trace domain filtering on the Shaganappi 1998 2-D geotechnical survey, CREWES Research Report Vol. 11.
Henley, D.C., 1999c, Radial trace computational algorithms at CREWES, CREWES Research Report Vol. 11.
Henley, D.C., 2000a, Wavefield separation in the radial trace domain, Geo-Canada 2000, Expanded Abstract No. 131
Henley, D.C., 2000b, More radial trace domain applications, CREWES Research Report, Vol. 12.
Henley, D.C., 2003, Coherent noise attenuation in the radial trace domain, Geophysics, Vol. 68, No. 4, pp 1408-1416.

FIGURES
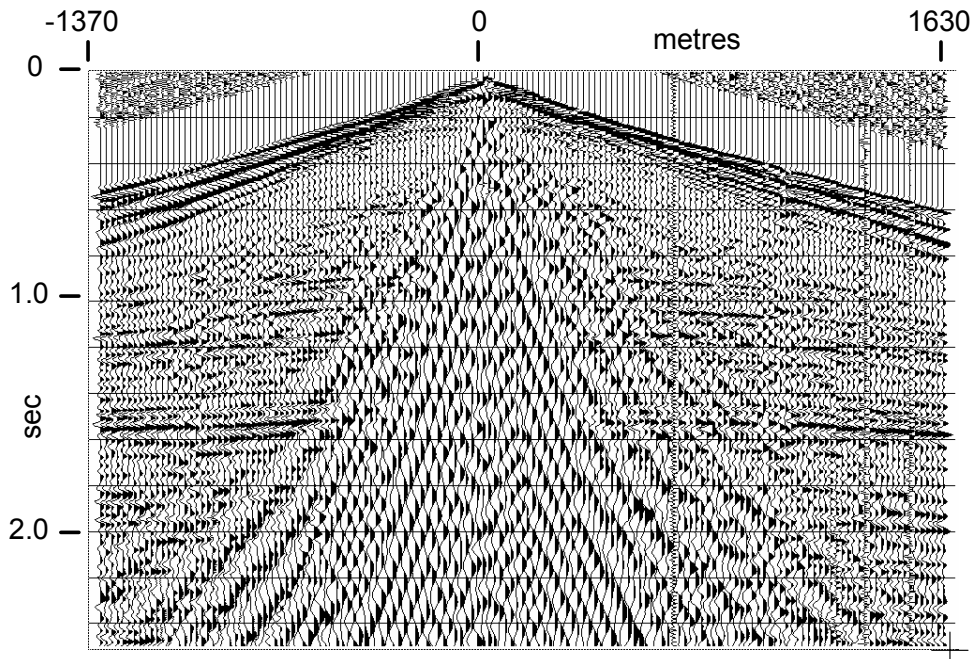
FIG. 1. Raw shot gather from the Blackfoot 2D survey, used exclusively in this report
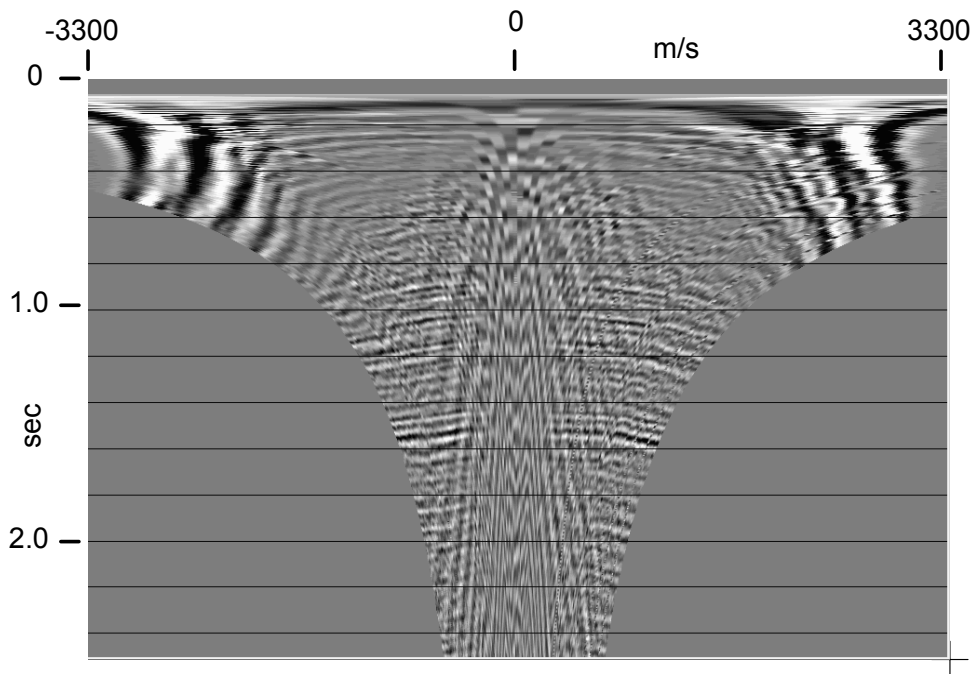
FIG. 2. R-T fan transform of raw Blackfoot shot gather
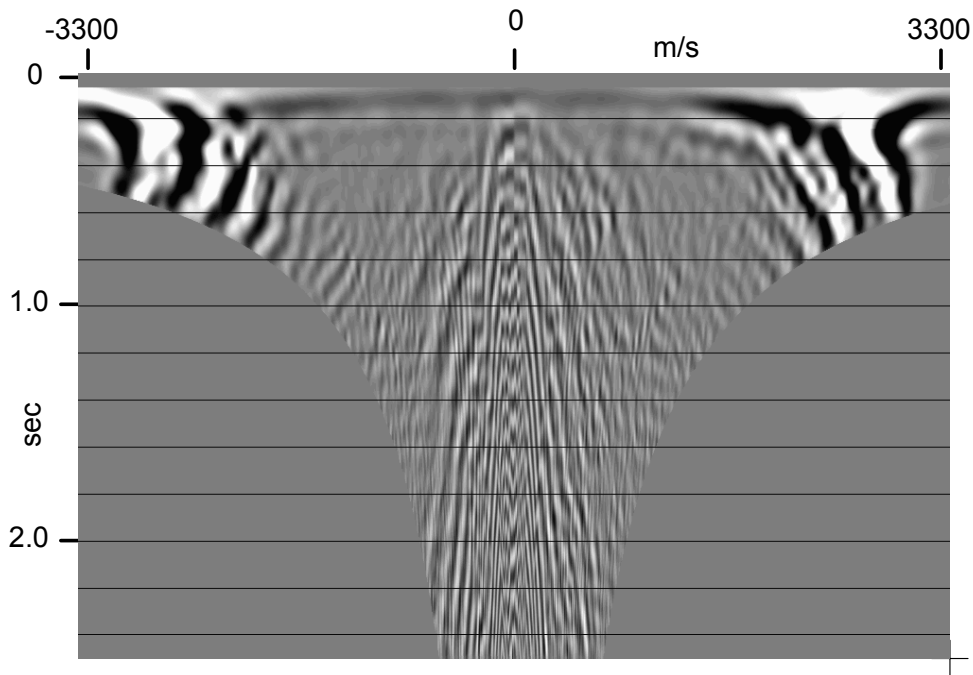
FIG. 3. Low-pass filtered R-T transform of raw Blackfoot shot gather.
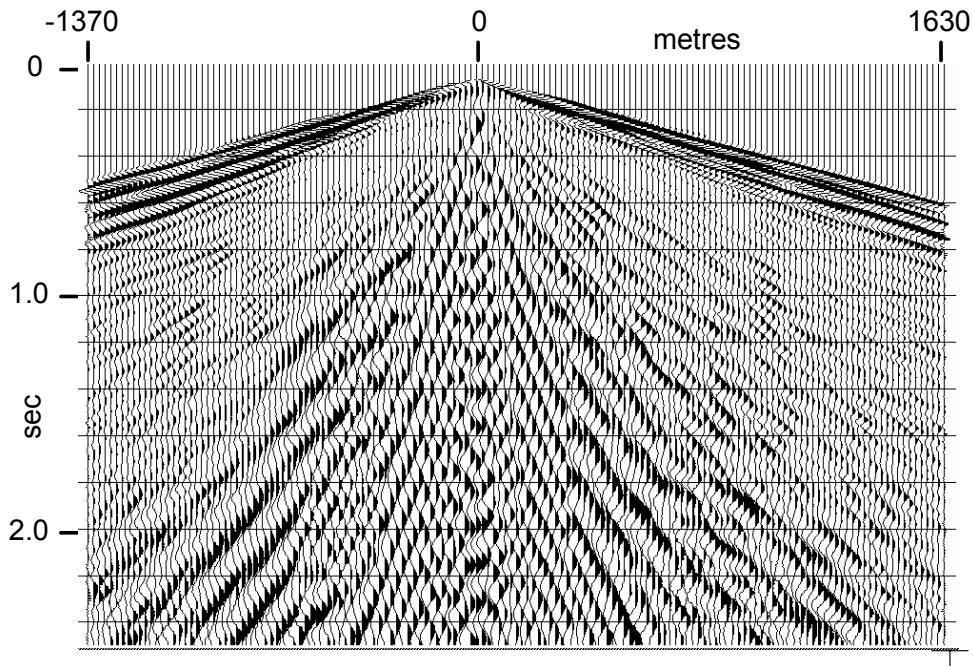
FIG. 4. Inverse transform of low pass filtered R-T transform in Figure 3—the 'modelled' coherent noise.
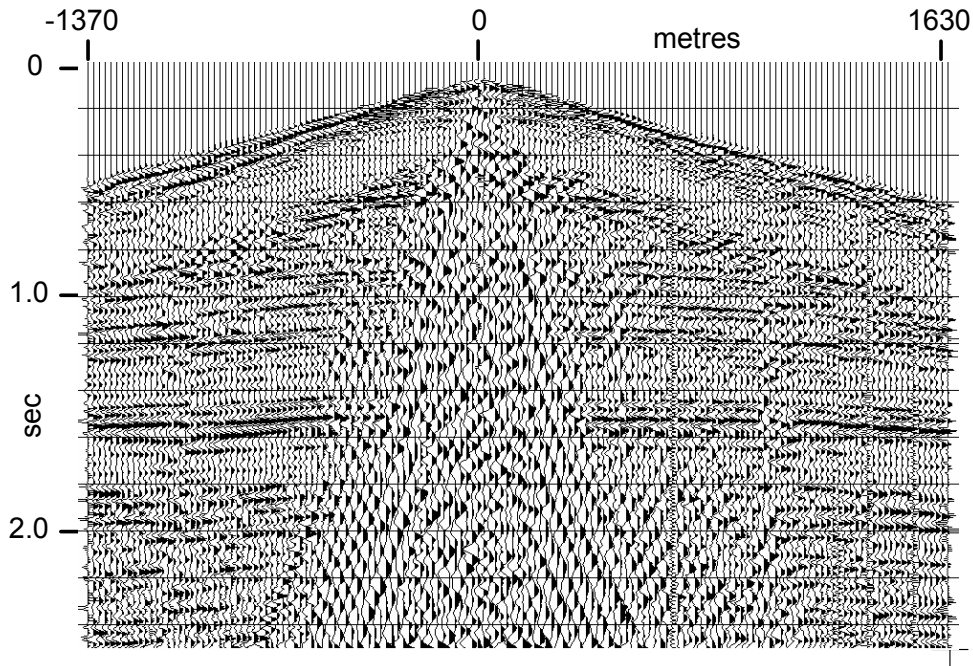
FIG. 5. Blackfoot shot gather after subtraction of modelled noise in Figure 4.
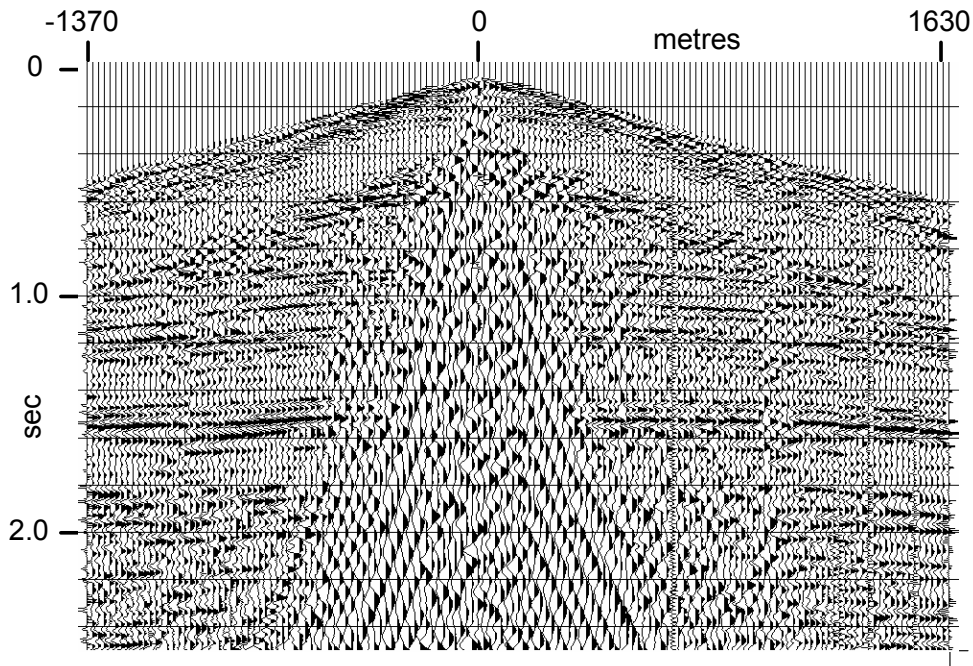
FIG. 6. Blackfoot shot gather after subtraction of modelled noise with a weight factor of 1.25. Direct arrivals somewhat more attenuated than in Figure 5.
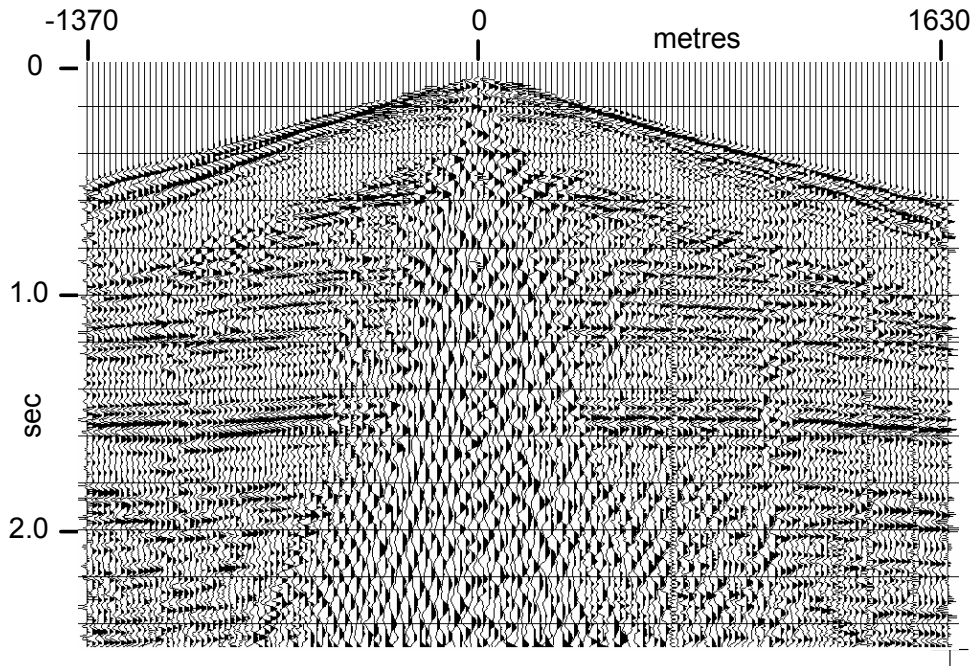
FIG. 7. Blackfoot shot gather after subtraction of modelled noise with weight factor of 0.8.
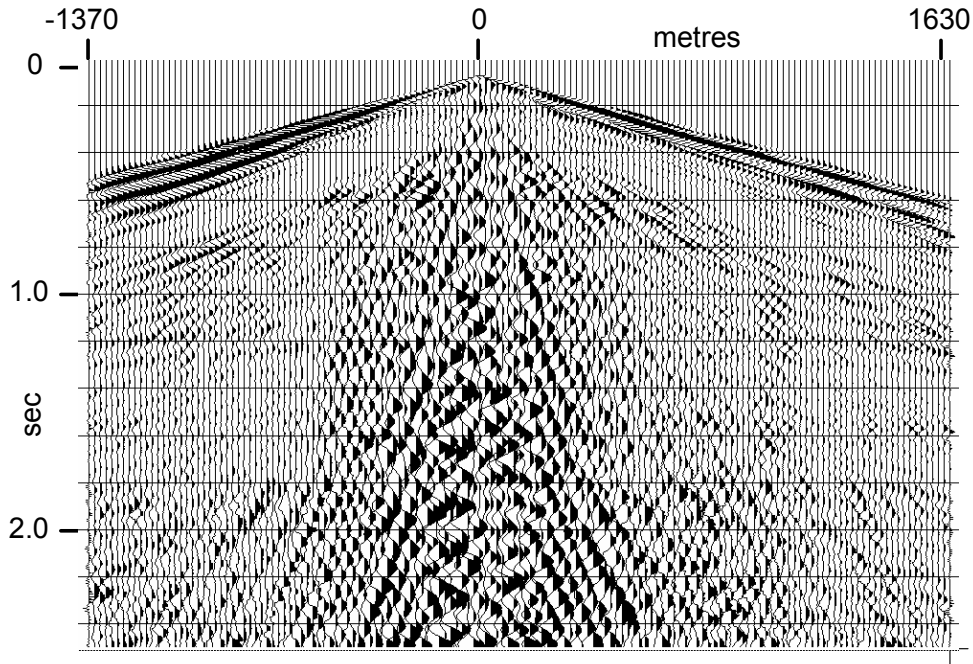
FIG. 8. Modelled noise from second iteration of R-T modelling.
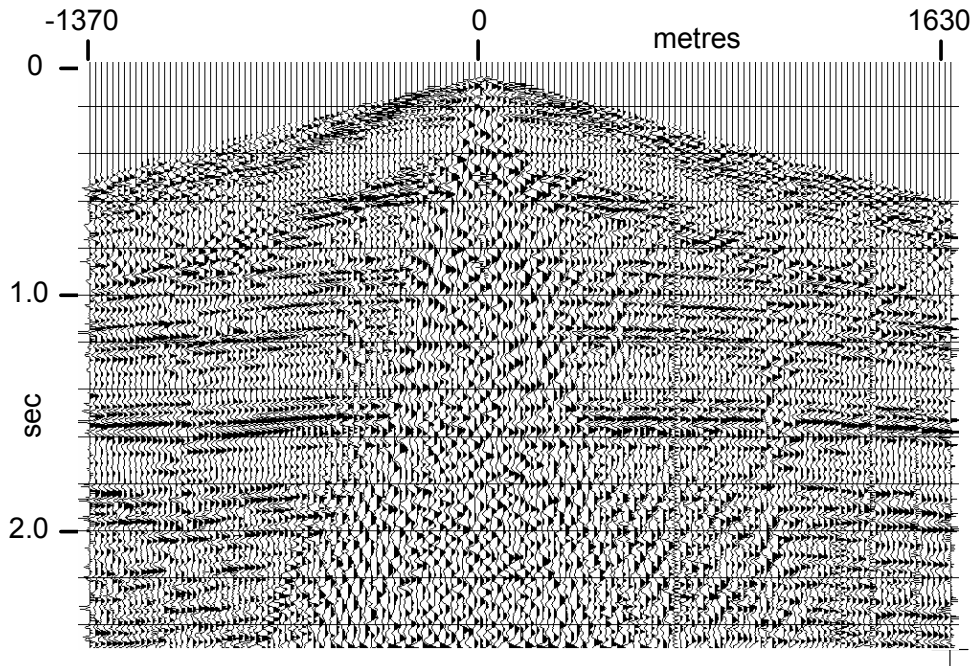
FIG. 9. Blackfoot shot gather after subtraction of first two estimates of modelled coherent noise.
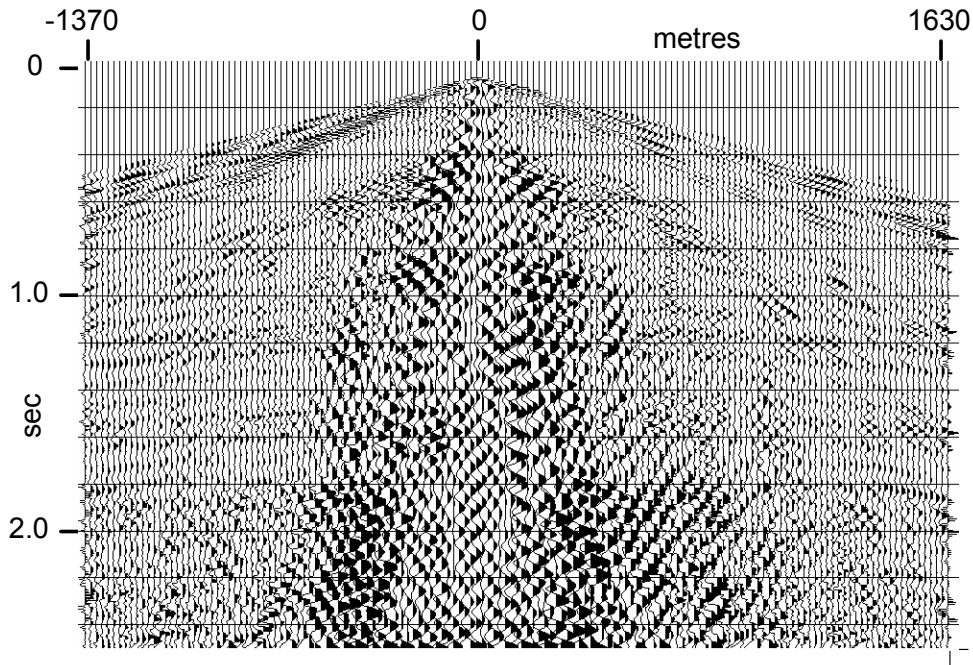
FIG. 10. Modelled coherent noise from fourth iteration of R-T modelling.
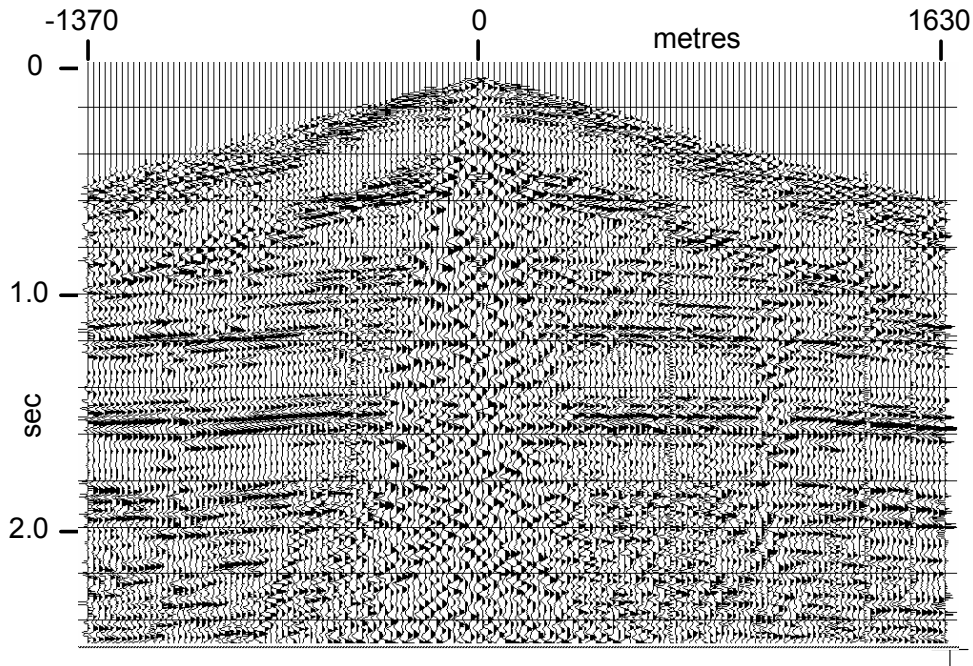
FIG. 11. Blackfoot shot after subtraction of coherent noise estimates from first four iterations of R-T modelling.
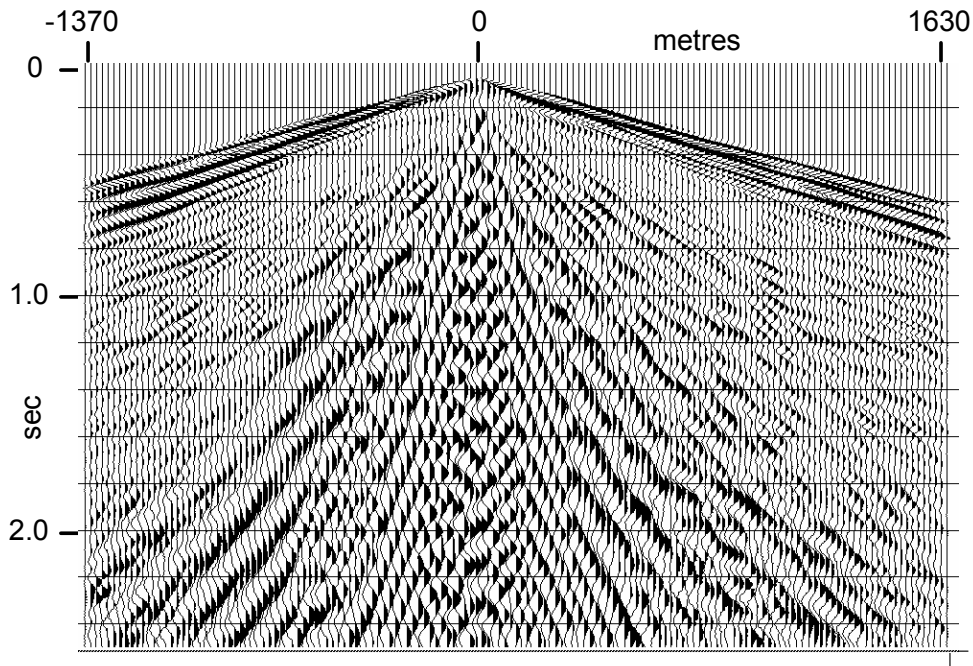
FIG. 12. Blackfoot noise estimate from four consecutive low pass filter applications in the R-T domain.
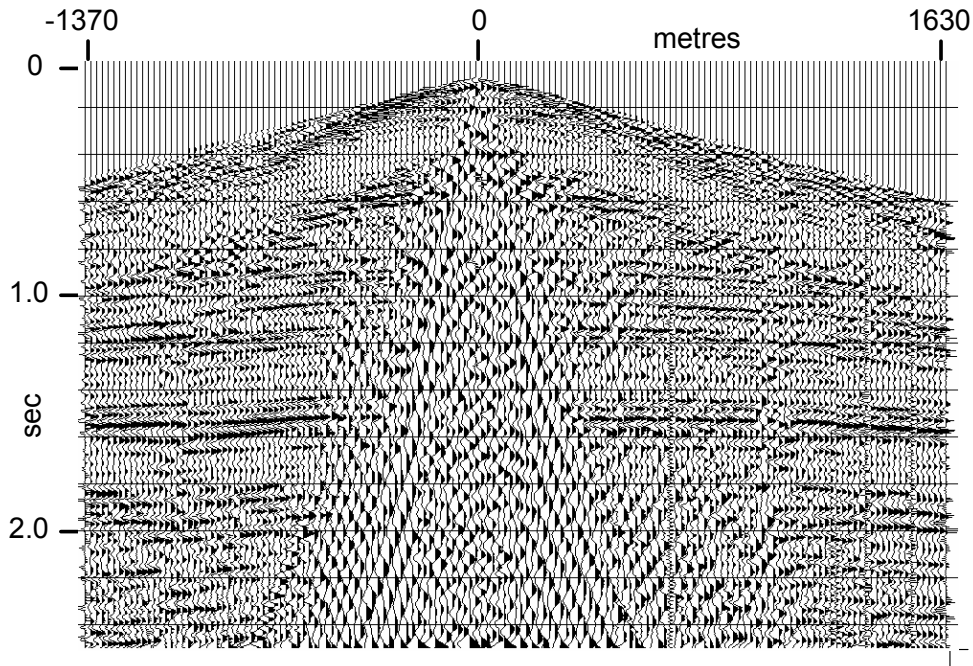
FIG. 13. Blackfoot shot gather after subtraction of noise modelled by four consecutive low-pass filters of R-T transform.
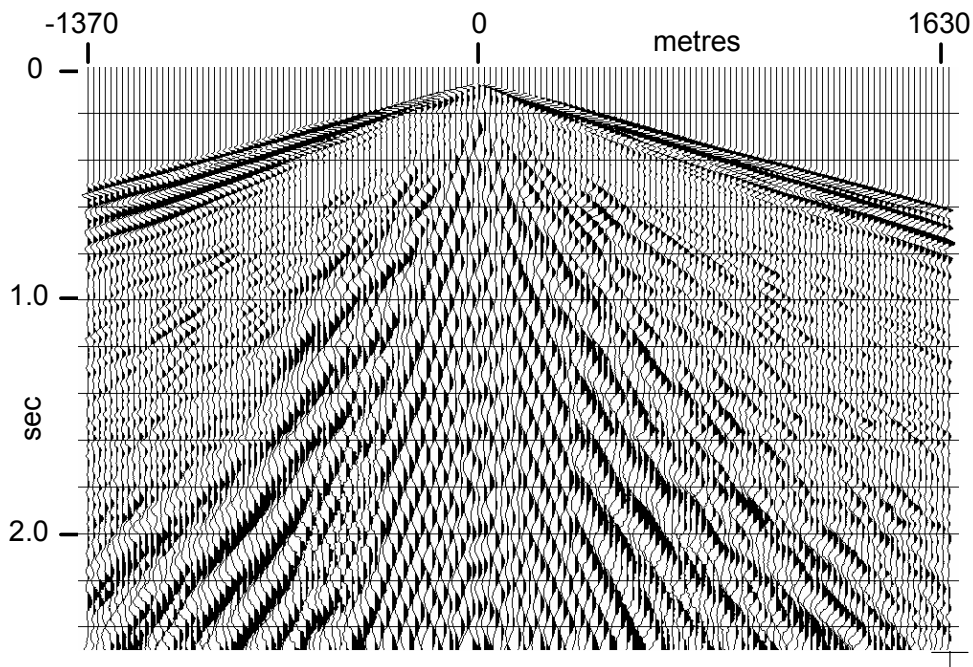
FIG. 14. Coherent noise from Blackfoot shot modelled by 100-point running mean applied in R-T domain.
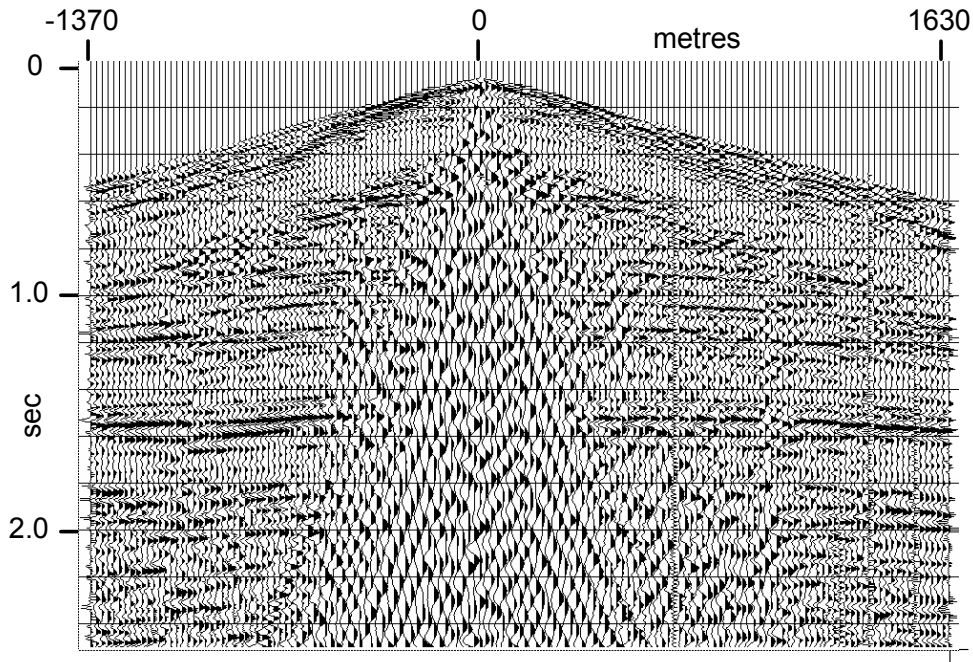
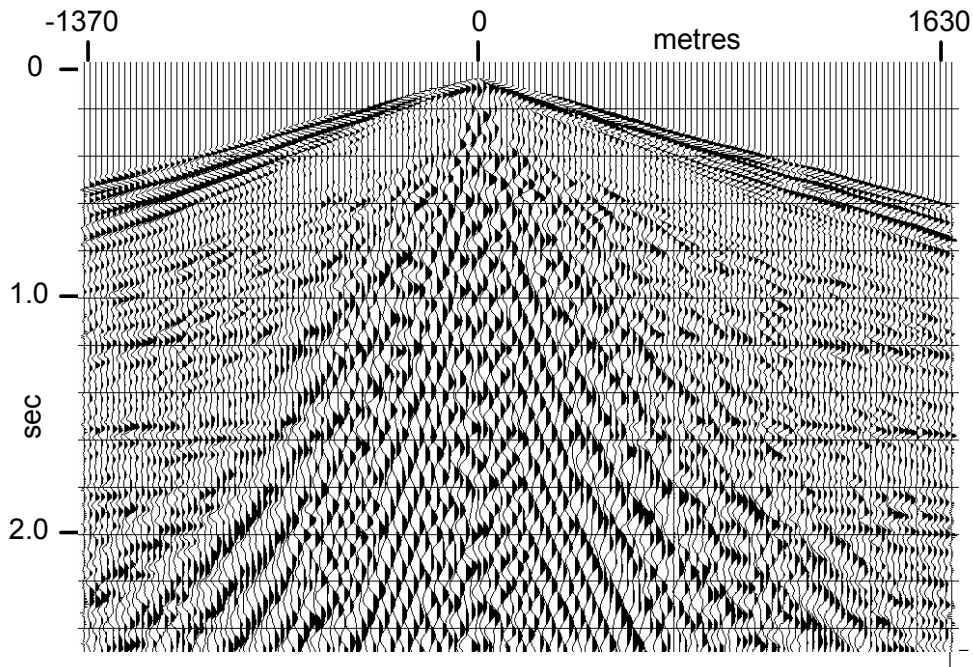FIG. 15. Blackfoot shot after subtraction of coherent noise modelled using 100-point running mean in R-T domain.
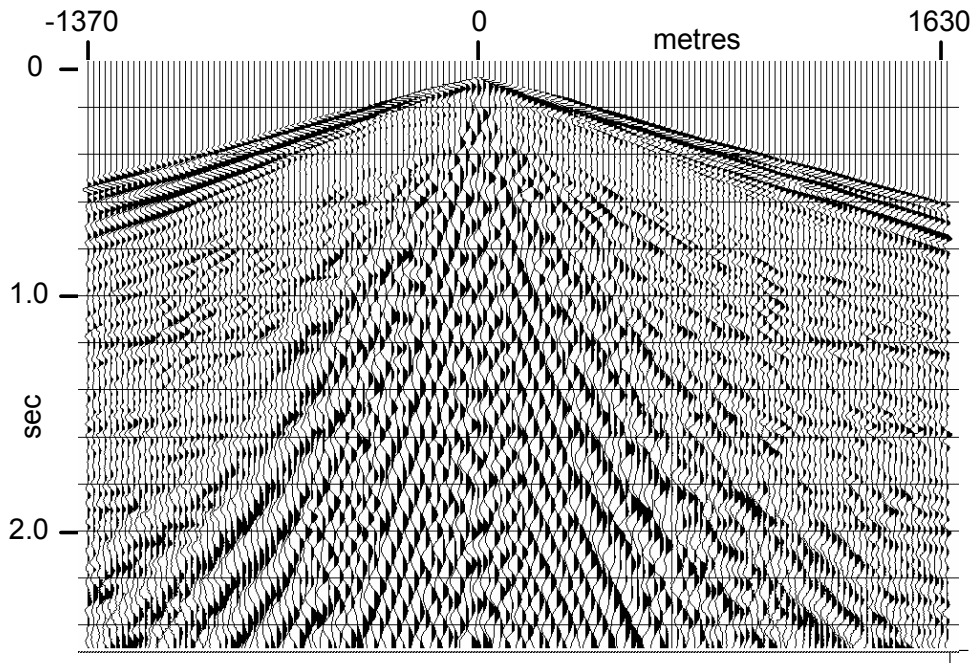
FIG. 16. Coherent noise modelled using 50-point running mean in R-T domain.
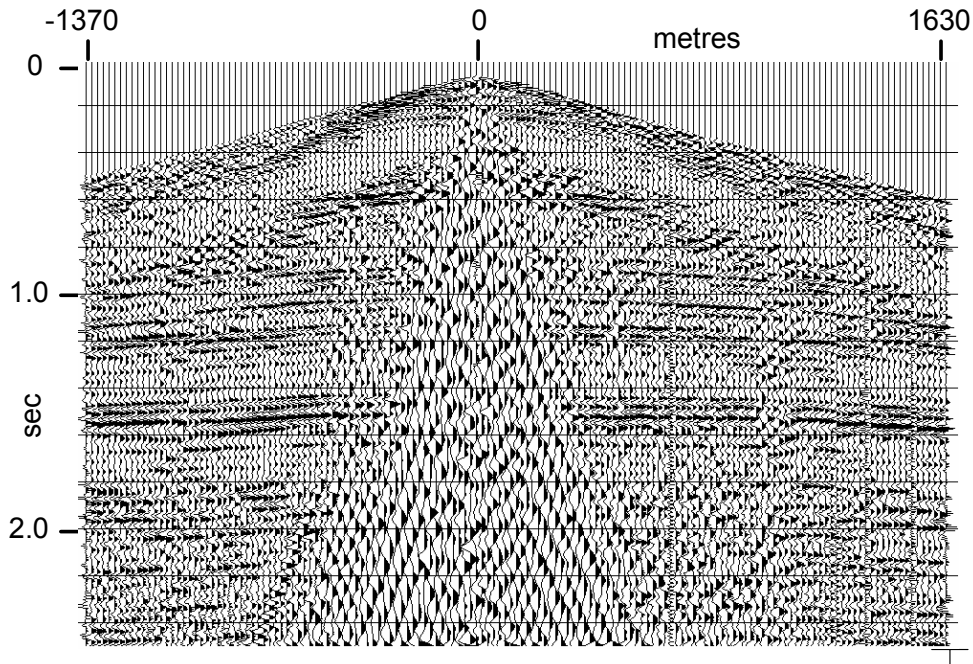
FIG. 17. Blackfoot shot after subtraction of coherent noise modelled using 50-point running mean in the R-T domain.
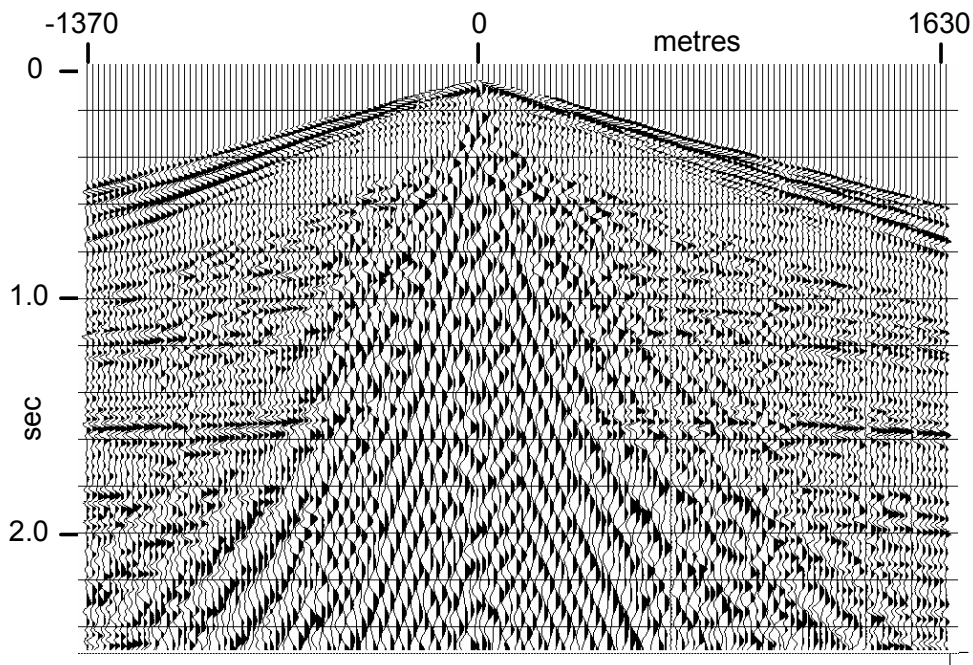
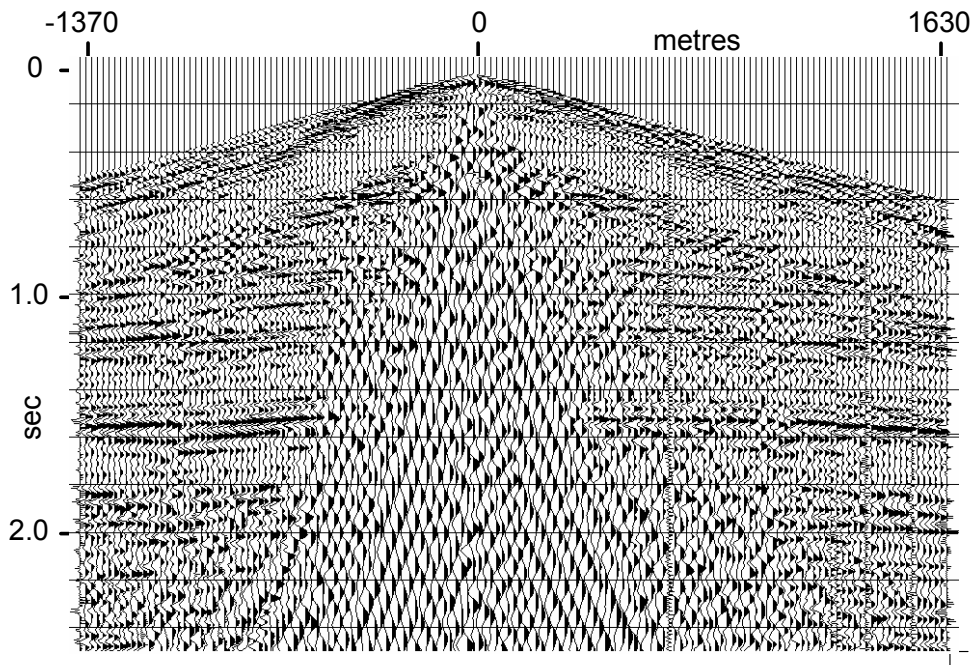FIG. 18. Coherent noise estimated using 25-point running mean in the R-T domain. Note the leakage of much reflection energy into this estimate.
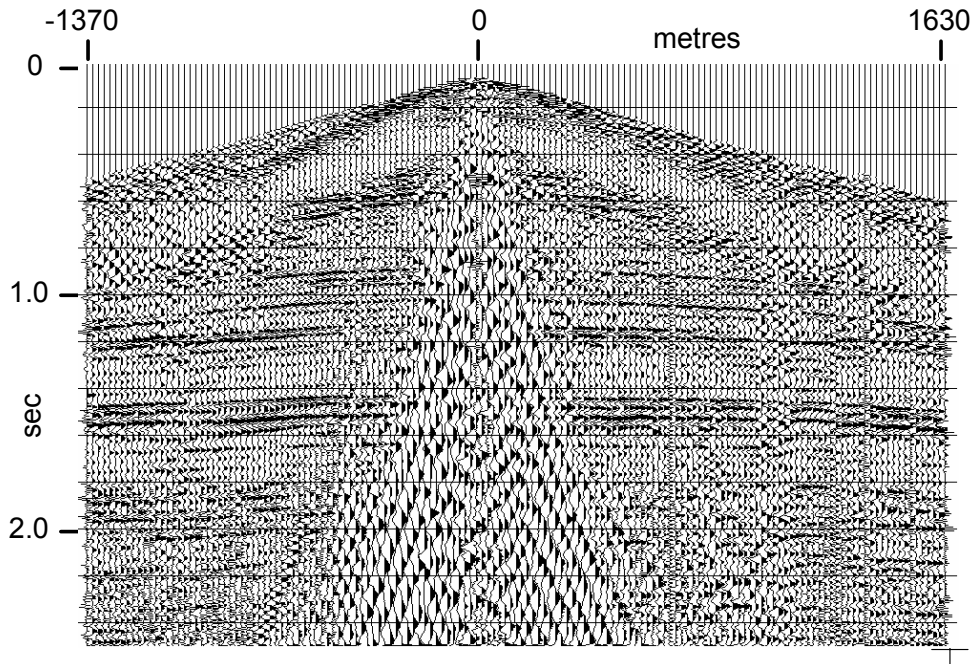
FIG. 19. Blackfoot shot after subtraction of noise estimate using 25-point running mean in R-T domain. Much energy lost from reflections in lower frequencies.
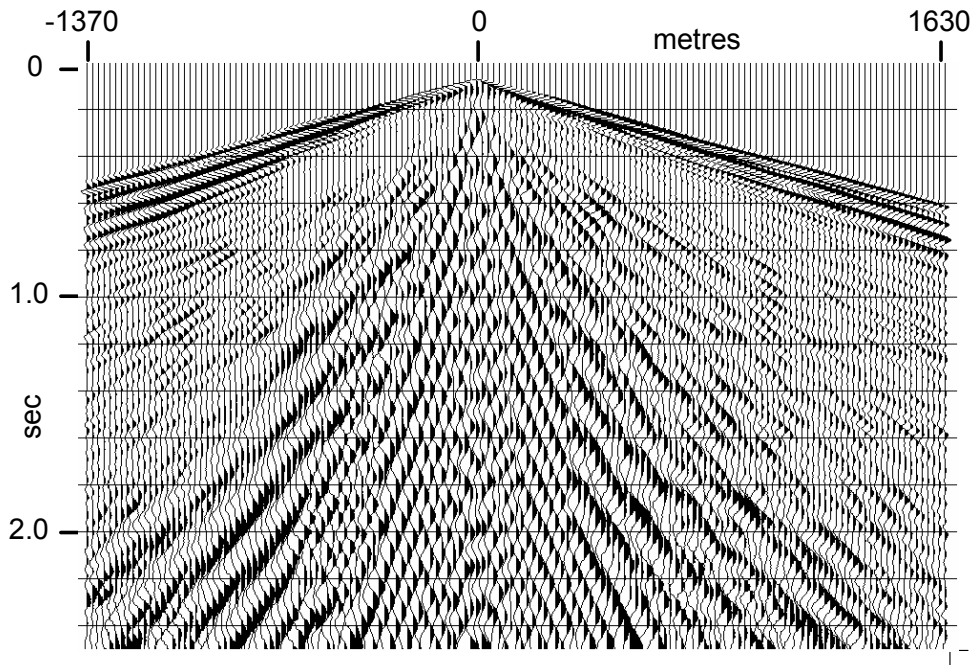
FIG. 20. Coherent noise estimate resulting from three consecutive passes of 50-point running mean in the R-T domain.
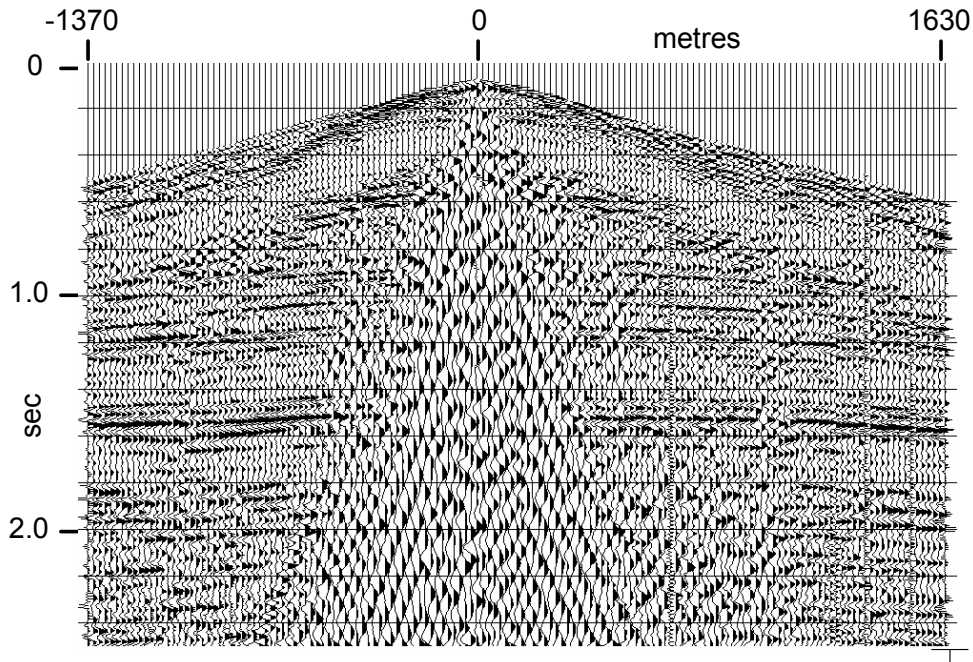
FIG. 21. Blackfoot shot after subtraction of noise estimate using three passes of 50-point running mean in R-T domain.
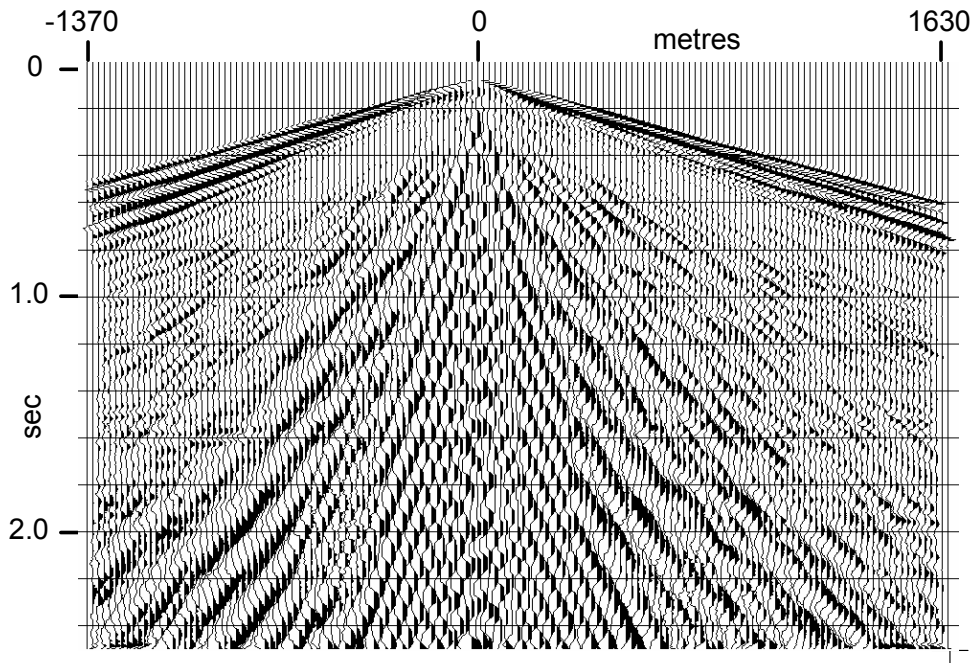
FIG. 22. Coherent noise estimate made using 100-point running median in the R-T domain. Note some clipping on the low-frequency waveforms in the central low-velocity portion of the noise.
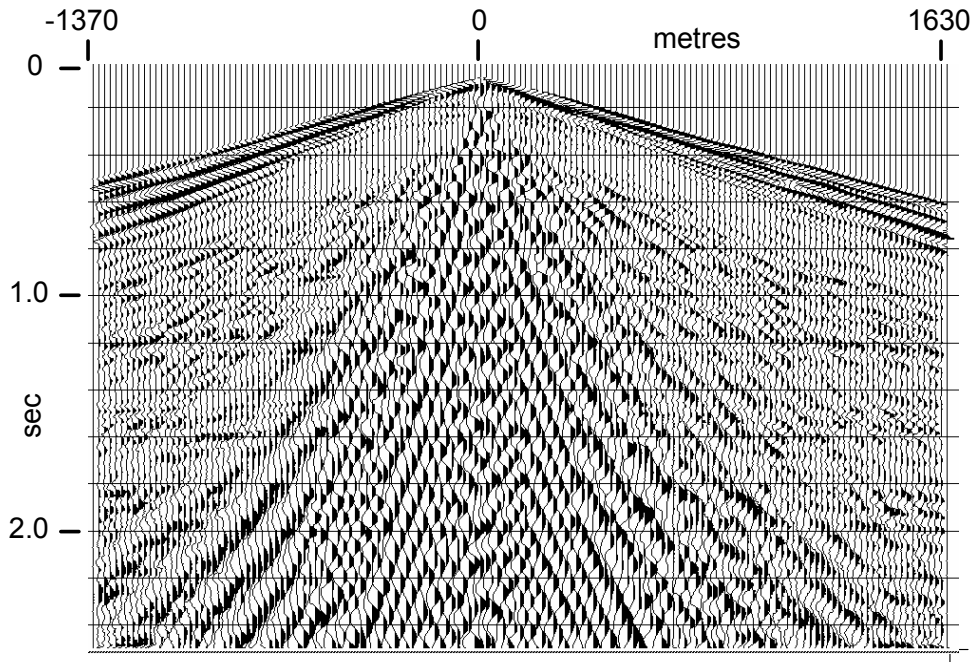
FIG. 23. Coherent noise estimate made using 50-point running median in the R-T domain. Note leakage of reflection energy into this estimate.
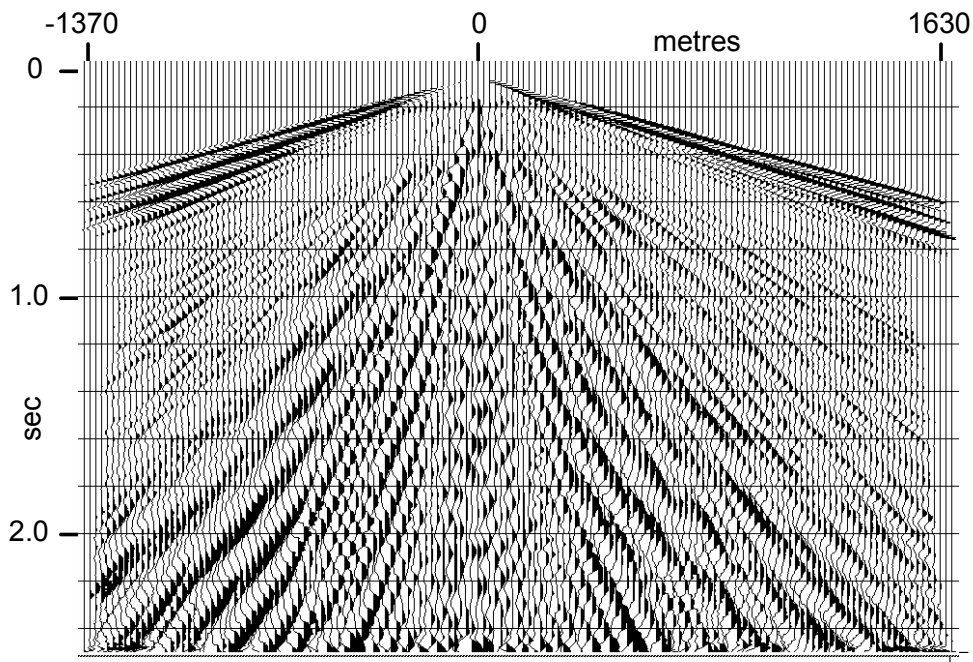
FIG. 24. Coherent noise estimate resulting from 300 point running median in the R-T domain.
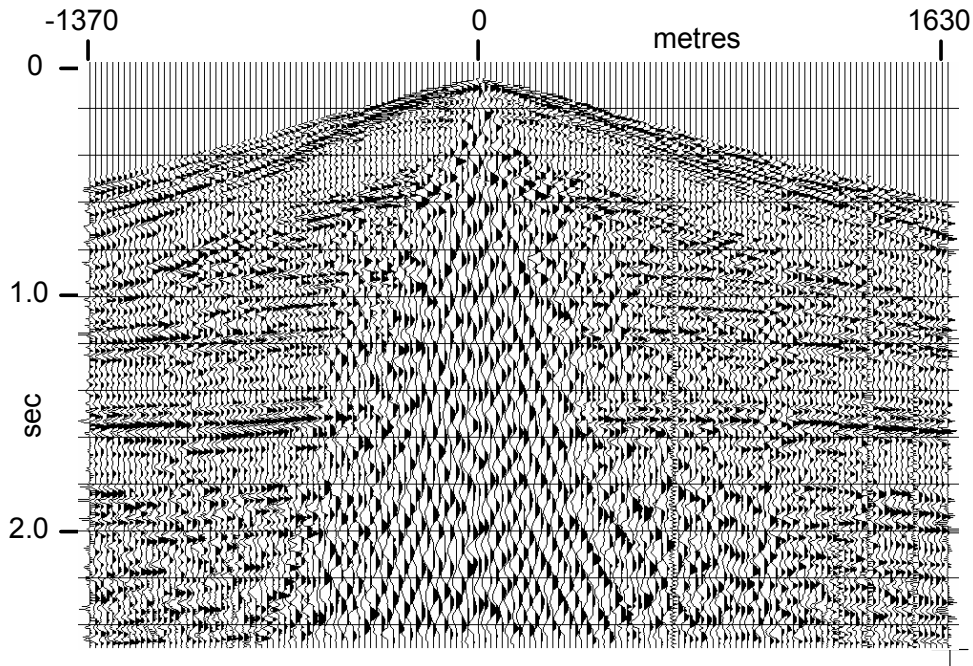
FIG. 25. Blackfoot shot after subtraction of coherent noise estimate using 300-point running median in the R-T domain.

FIG. 26. Coherent noise estimate resulting from application of K-F filter in the R-T domain. Note leakage of reflection energy.
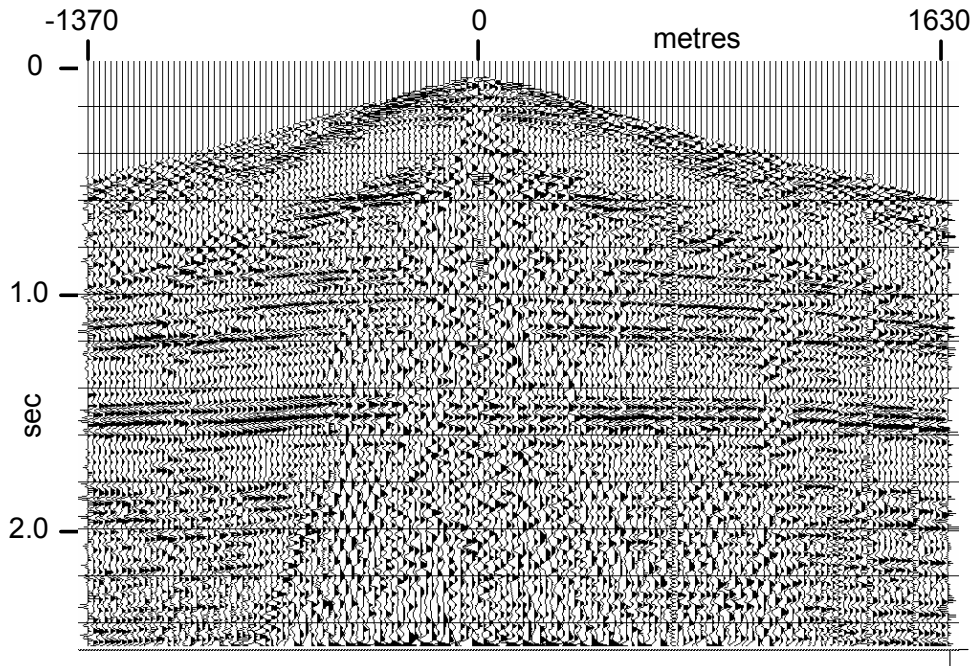
FIG. 27. Blackfoot shot after subtraction of coherent noise estimated using K-F filter in the R-T domain. Note relative effectiveness of noise reduction in the centre of the record, loss of some lower frequencies in the reflections.
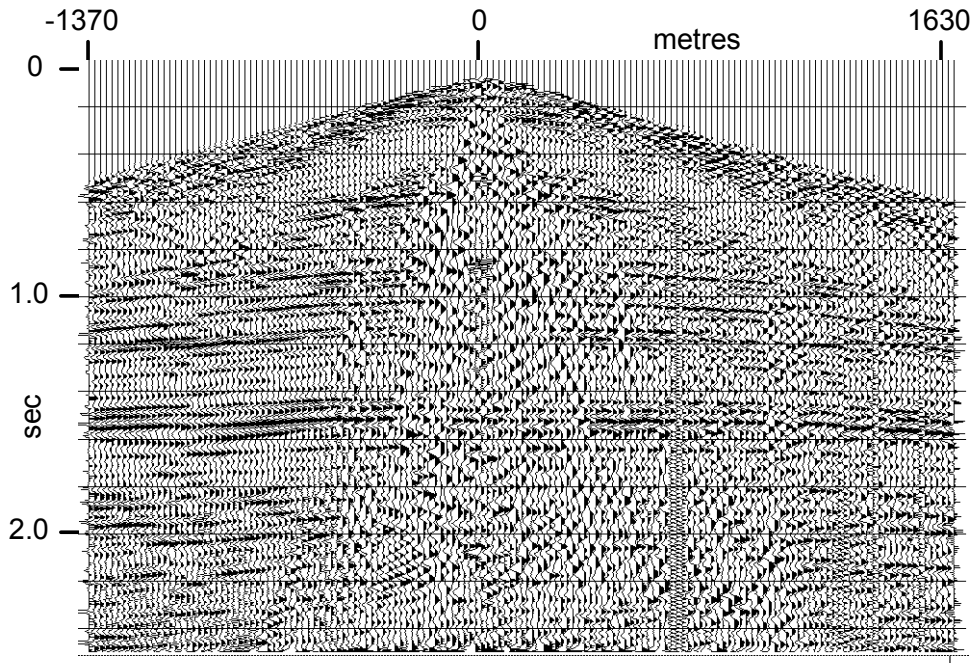
FIG. 28. Blackfoot shot with noise attenuated directly using a K-F filter in the R-T domain. Note lateral smearing, particularly on 60 Hz trace in right hand part of spread at deeper times.
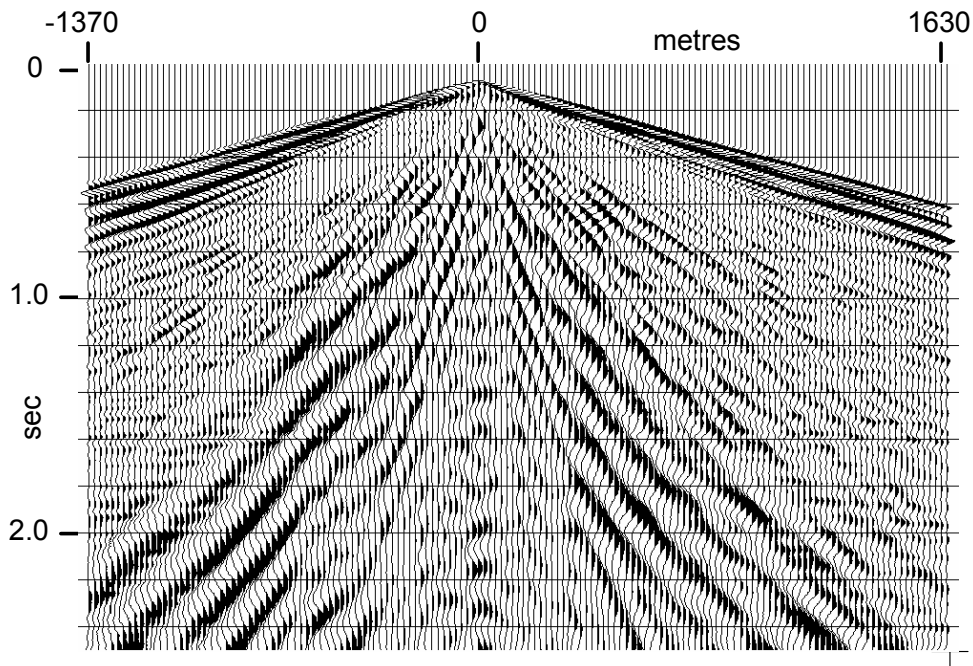
FIG. 29. Coherent noise estimate obtained using 2D moving average in the R-T domain.

FIG. 30. Blackfoot shot after subtraction of coherent noise modelled using 2D running mean in the R-T domain.
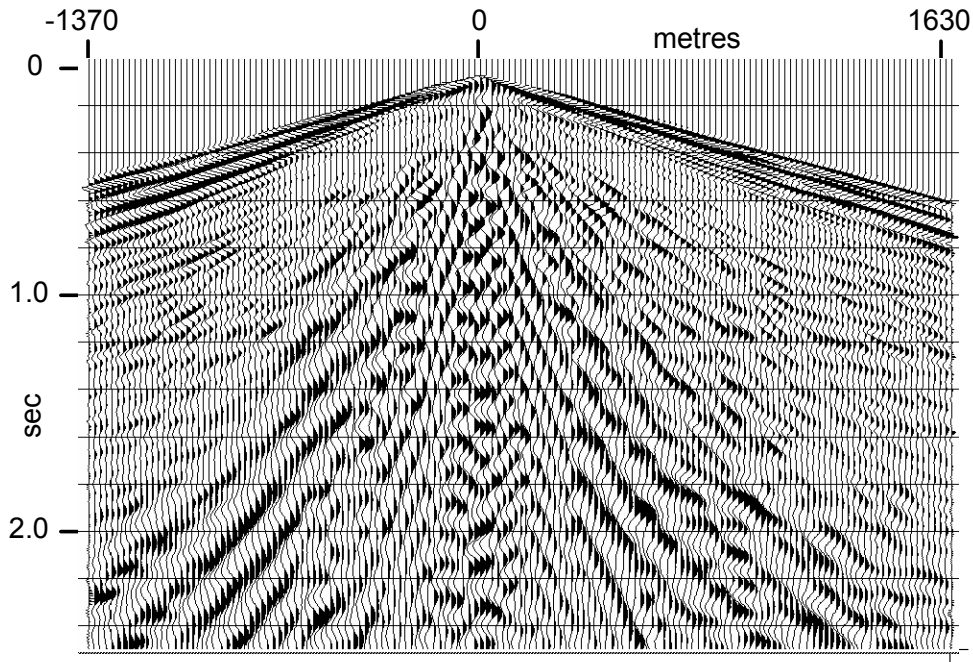
FIG. 31. Coherent noise estimate obtained using a weighted trace mix and low-pass filter in the R-T domain.
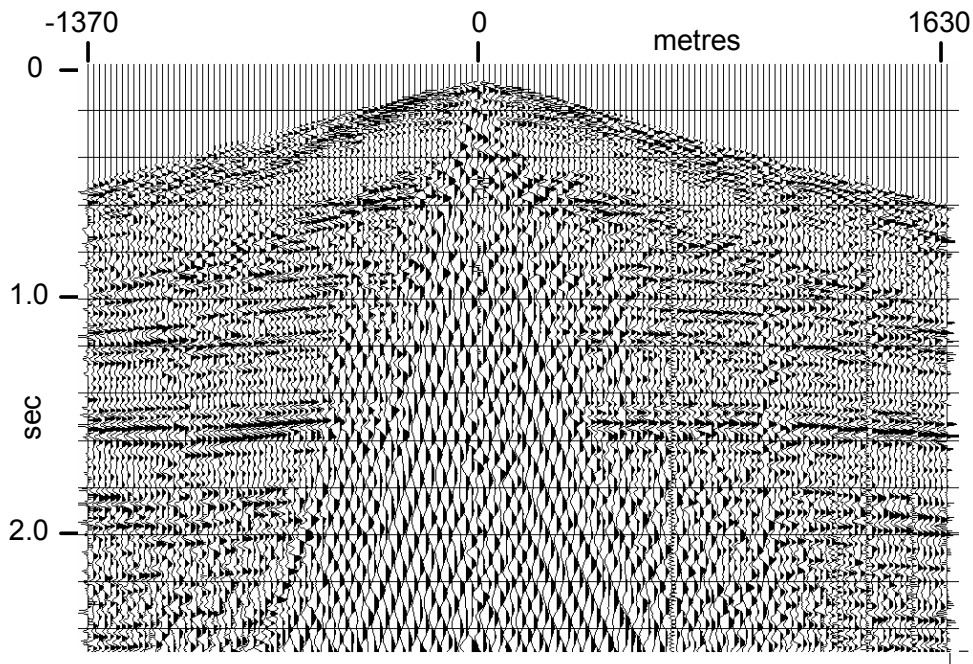
FIG. 32. Blackfoot shot gather after subtraction of noise estimate obtained using weighted trace mix and low-pass in the R-T domain.
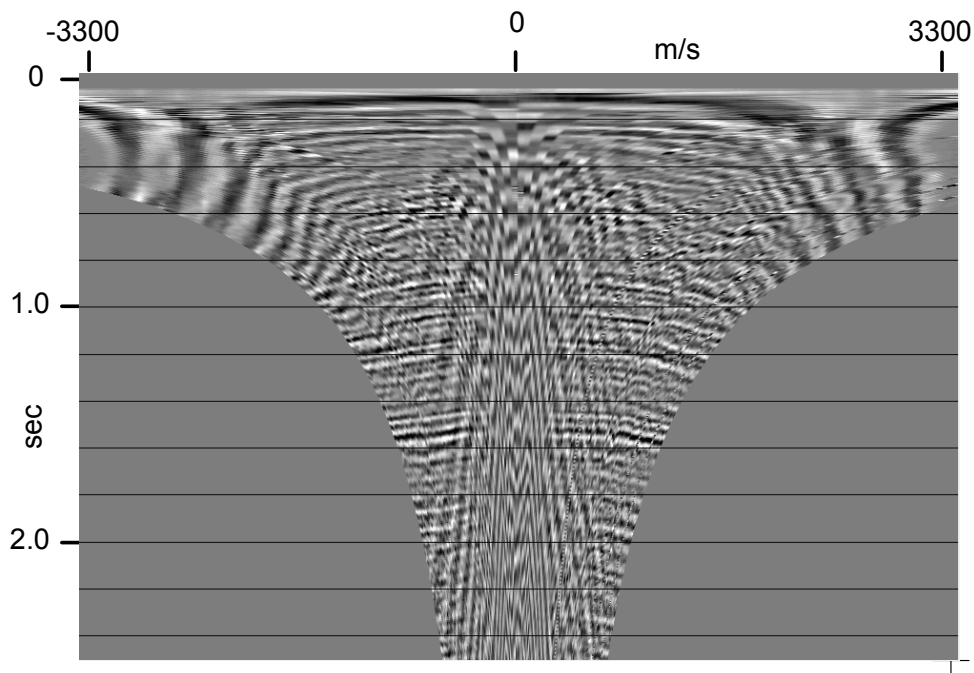
FIG. 33. Linear R-T transform of Blackfoot shot gather (R-T trajectories are constant velocity)
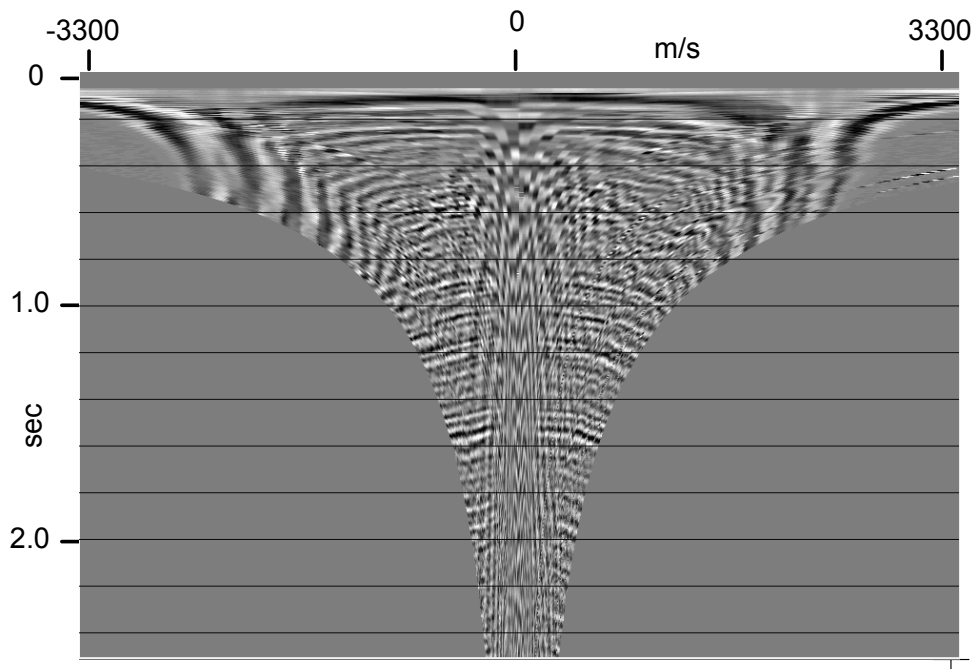
FIG. 34. R-T transform of Blackfoot shot gather using curved R-T trajectories (velocity of each trajectory increases 50% per second)
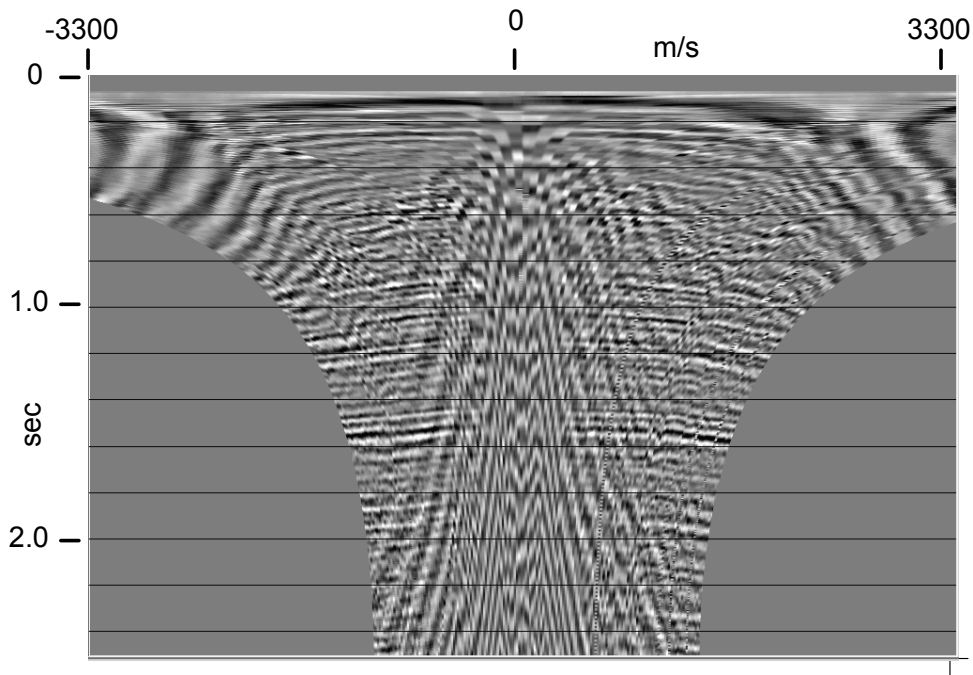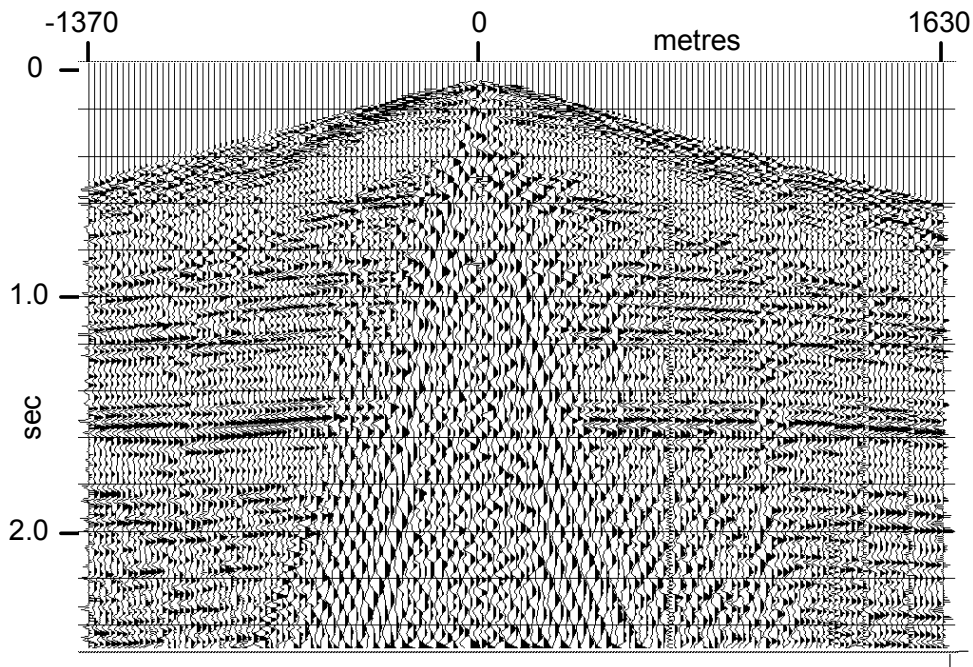
FIG. 35. R-T transform of Blackfoot shot gather using curved R-T trajectories (velocity of each trajectory decreases 20% per second).

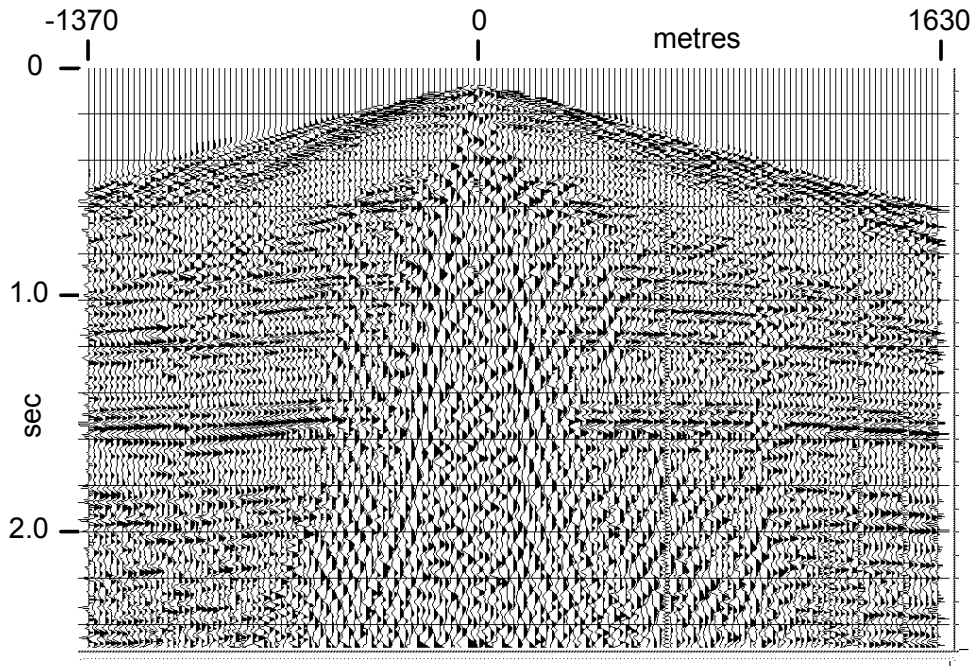FIG. 36. Blackfoot shot after low cut in R-T domain using linear R-T trajectories from Figure 33.

FIG. 37. Blackfoot shot after low cut in R-T domain using curved R-T trajectories from Figure 34.
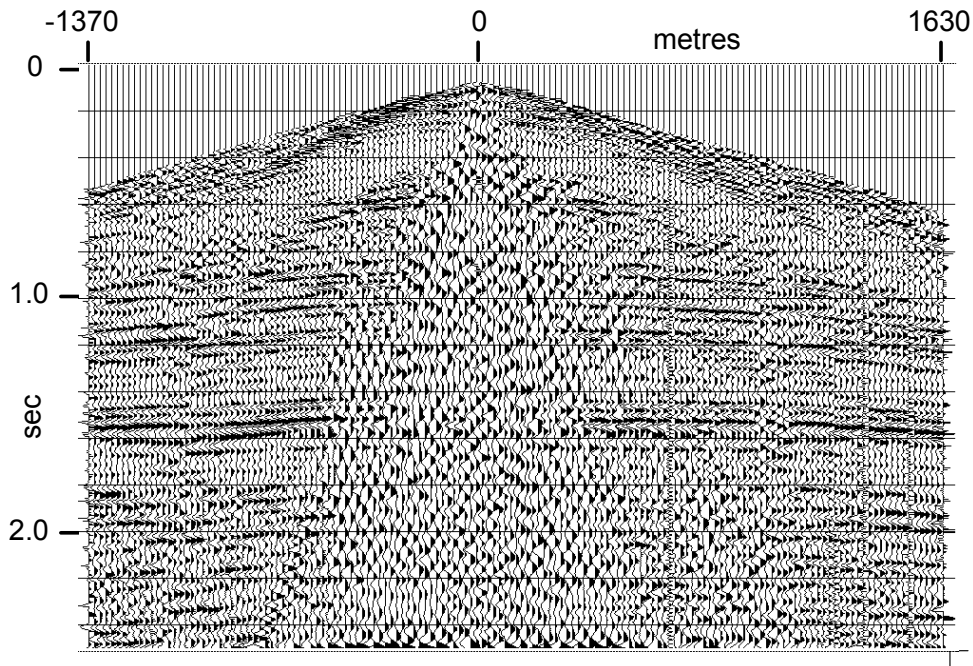

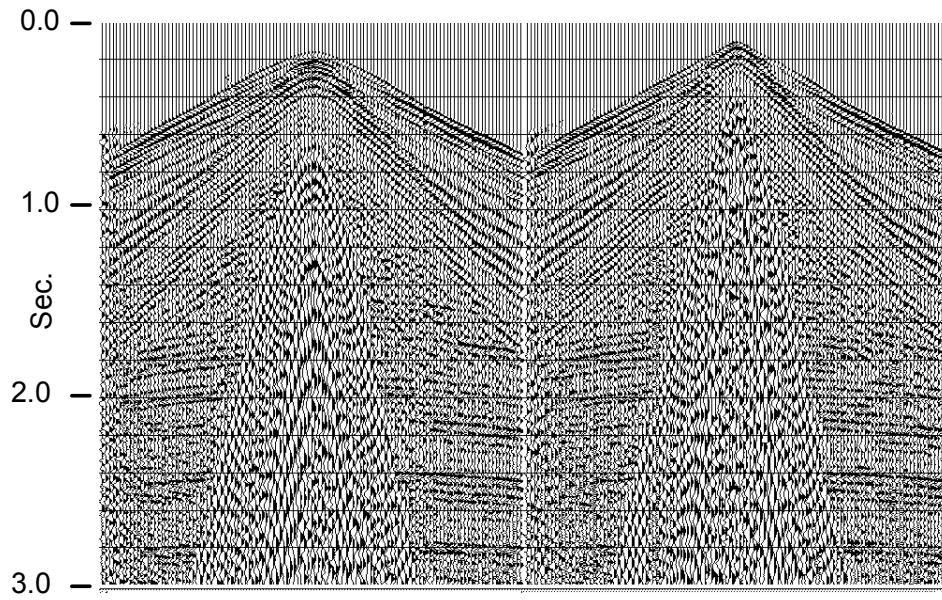FIG. 38. Blackfoot shot after low cut in R-T domain using curved trajectories from Figure 35.

FIG. 39. Two receiver-line gathers from a 3D land survey with abundant source-generated noise.
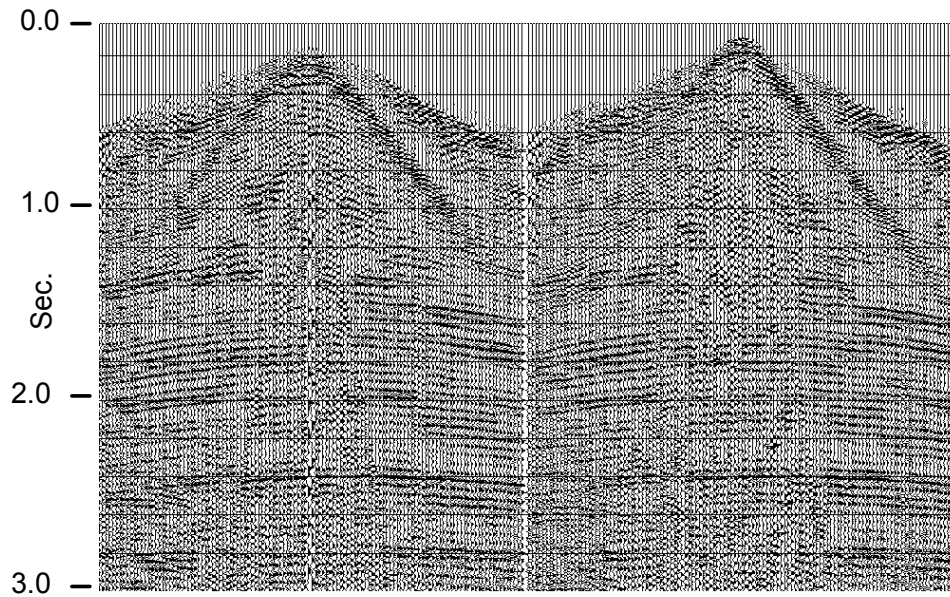

FIG. 40. 3D receiver-line gathers after application of R-T domain coherent noise attenuation.